Characterize the magnetic signal generated in the magnetosphere from geomagnetic observations

Yalei Shi, Vincent Lesur, Erwan Thébault

Characterize the magnetic signal generated in the magnetosphere from geomagnetic observations

Yalei SHI[1], Vincent LESUR[1], Erwan THEBAULT[2]

[1]Université Paris Cité, Institut de physique du globe de Paris, CNRS F-75005 Paris, France
[2]Université Clermont-Auvergne, Laboratoire Magmas et Volcans, CNRS F-63170 Aubière, France

Introduction

The main contribution to the geomagnetic field is from the core, but fields generated from the magnetosphere during magnetically quiet periods play an important role. They may have geomagnetic contributions up to hundreds of nanoteslas (nT) during magnetic storm. To study the geomagnetic field, the contributions from different sources need to be separated and modeled. In current models of the geomagnetic field derived from satellite data, the magnetospheric components are poorly described because of the limitation of satellite data spatiotemporal resolution. The poorly described magnetospheric component limits the resolution of other geomagnetic contributing sources, especially the contributions from the core (Thebault et al. [2011]) and the lithosphere (Lesur et al. [2013]). It is therefore important and necessary to describe and model precisely the magnetospheric components. We describe here an approach for their modeling based on Kalman filter approach and magnetic observatory data. These provide a data set with a temporal resolution particularly well suited to characterize rapidly varying magnetospheric signals.

Objective:

- Study the magnetospheric field up to spherical harmonic (SH) degree 6 (L=6) through normal distributions ($\mathcal{N}(\mu = \mathrm{m}, \sigma^2 = C_m)$) with a time resolution of an hour, based on a Kalman filter and correlation-based modeling.

Test models with synthetic data

Synthetic data at each observatory include only magnetospheric field signal and its response in the mantle:

1), generation of a random hourly sequence during the whole 2021 year for each Gauss coefficient q_l^m up to degree L=6

2), removal of the principal trend by PCA and normalization of the random distribution of q_l^m by the variance trends from the IGRF-13 field power spectrum

3), generation of i_l^m by multiplying the normalized q_l^m with a 1D electrical conductivity model (Verhoeven, Thebault, Saturnino, Houliez, and Langlais [2021])

Night synthetic data (23:00 – 05:00 LT)

Full-year synthetic data

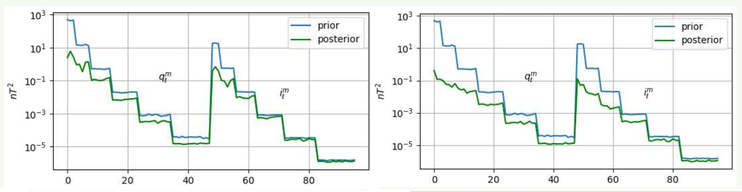

Figure 2: The left: results by fitting only night synthetic data. The right: results by fitting full-year synthetic data.
Top: The diagonal elements of the model covariance matrix
Bottom: Power spectrum of SH Gauss coefficient as a function of SH degree

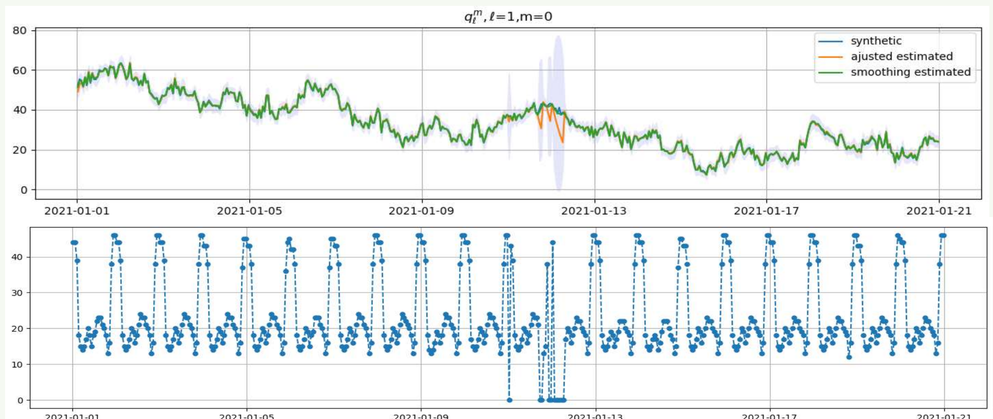

Figure 3: Top: View of a comparison during the first 20 days between synthetic Gauss coefficient (blue) and the estimated $\boldsymbol{q_1^0}$ (orange and green) by fitting only synthetic data at night (23:00 – 05:00) with error bar 3σ (lavender). Bottom: the number of used data at each hour

Future works

- The hourly model needs to be extended to cover 1999 to 2024
- Improvement of hourly model: observatory data including day side should be used. The ionospheric contribution distribution of each component at each observatory should be co-estimated, and a correlation of ionospheric contribution among observatories should be added as a priori information
- Statistics from theoretical or semi-empirical models to separate the different contributions in the magnetosphere could be used, in order to develop a better understanding of the evolution of magnetospheric sources during solar cycles

References

1. Thebault E., Vervelidou F., Lesur V., & Harmoudi M. (2011). The pros and cons of along-track satellite analysis in planetary magnetisme. In 25th IUGG General Assembly.
2. Lesur V., Rother M., Vervlidou F., Harmoudi M., Thebault E. (2013). Post-processing scheme for modelling the lithosphere magnetic field. Solid Earth, 4(1):105-118.
3. Ropp G., Lesur V., Baerenzing J., & Holschneider M. (2020), Sequential modelling of the earth's core magnetic field. Earth, Planets and Space, 72(1):1-15.
4. Verhoeven, O., Thebault, E., Saturnino, D., Houliez, A., & Langlais, B. (2021). Electrical conductivity and temperature of the earth's mantle inferred from bayesian inversion of swarm vector magnetic data. Physics of the Earth and Planetary Interiors, 314, 106702.

INTERMAGNET observatory data

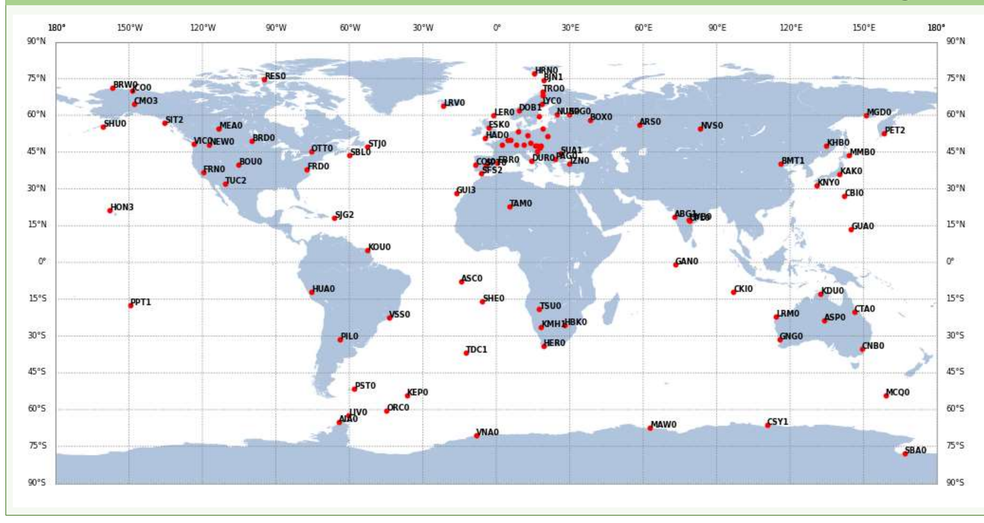

1, The main magnetic field contribution is removed from the hourly-mean INTERMAGNET observatory data for full-year 2021 by subtracting the MCM model (Ropp et Lesur [2020])
2, Observatory data are selected between 23:00 - 05:00 LT and during geomagnetically quiet time (Dst between -30 nT and 30 nT) to minimize the contributions of ionospheric perturbations

Figure 1: Distribution of the hundred or so used geomagnetic observatory positions

Parameters

The geomagnetic signal after the selection is considered as the sum of the magnetospheric field, induced field, and crustal offsets at each observatory location:

$$B(r,\theta,\phi) = \sum_{\ell,m} q_\ell^m \left(\frac{r}{a}\right)^{l-1} Y_\ell^m(\theta,\phi) + \sum_{\ell,m} i_\ell^m \left(\frac{a}{r}\right)^{l+2} Y_\ell^m(\theta,\phi) + \sum_{i \in N_{obs}} \delta(r-r_i, \theta-\theta_i, \phi-\phi_i) O_i$$

	magnetosphere	induced field	crustal offset
Coef.	q_ℓ^m	i_ℓ^m	$O_i=(O_x^i, O_y^i, O_z^i)$
m_0	0	0	O_i
C_0	$V_\ell^{ext}=R(\ell)=S(\frac{R}{a})^{2\ell}$	$0.3^2 V_\ell^{ext}$	~ 0
S	$0.7.10^4 (nT^2)$	-	-
R	$3.5.10^4$km	-	-
$\tau, (P=e^{-\frac{\Delta t}{\tau}})$	10 hour	10 hour	10^6 year
A	$\sum_{\ell,m}(\frac{r}{a})^{\ell-1} Y_\ell^m$	$\sum_{\ell,m}(\frac{a}{r})^{\ell+2} Y_\ell^m$	1
Nb. of par.	48	48	3×102

Approach -- Kalman Filter

- **Prior information:**
  mean prior model m_0, prior covariance matrix C_0
- **Analysis step:**
  adjustment of models at the ***k***th hour by fitting INTERMAGNET observatory data, based on the Least Square method

$$d = Am + \mathrm{e}$$
$$m_k^* = m_k + (A^t C_e^{-1} A + C_k^{-1})^{-1} A^t C_e^{-1} (d - Am_k)$$
$$C_k^* = (A^t C_e^{-1} A + C_k^{-1})^{-1}$$

- **Prediction step:**
  prediction of the next hour's model (at the ***(k+1)***th hour) based on the previous adjusted hourly model (at the ***k***th hour)

$$m_{k+1} = P m_k^*$$
$$C_{k+1} = P C_k P^t + C_w$$

- **Smoothing step:**
  a posteriori smoothing of the calculated series, based on conditioning rules of Gaussian distribution

$$m_k^s = m_k^* + G_k (m_{k+1}^s - m_{k+1})$$
$$C_k^s = C_k^* - G_k (C_{k+1} - C_{k+1}^s) G_k^t$$
$$G_k = C_k^* P^t C_{k+1}^{-1}$$

Results applied to real data

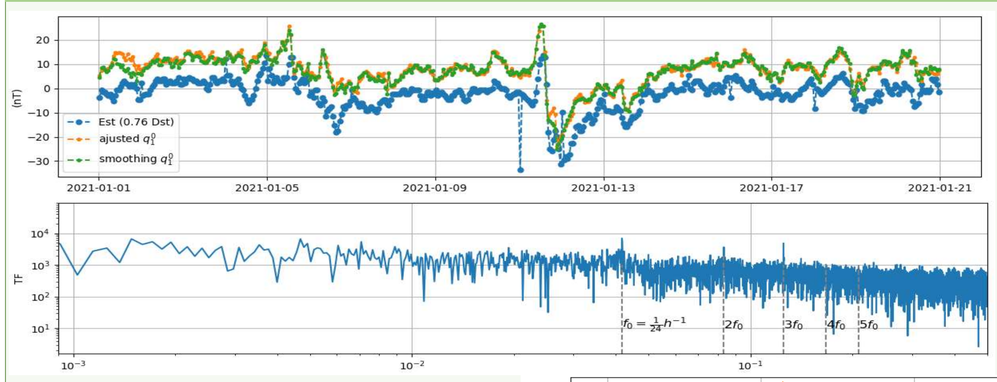

Figure 4: Top: Example of the comparison between **Dst** (in blue) and modeling $\boldsymbol{q_1^0}$ (orange, green) for 20 days
Bottom: Example of the difference between modeling $\boldsymbol{q_1^0}$ after smoothing step and **Dst** for the whole year 2021 in the Fourier transform domain

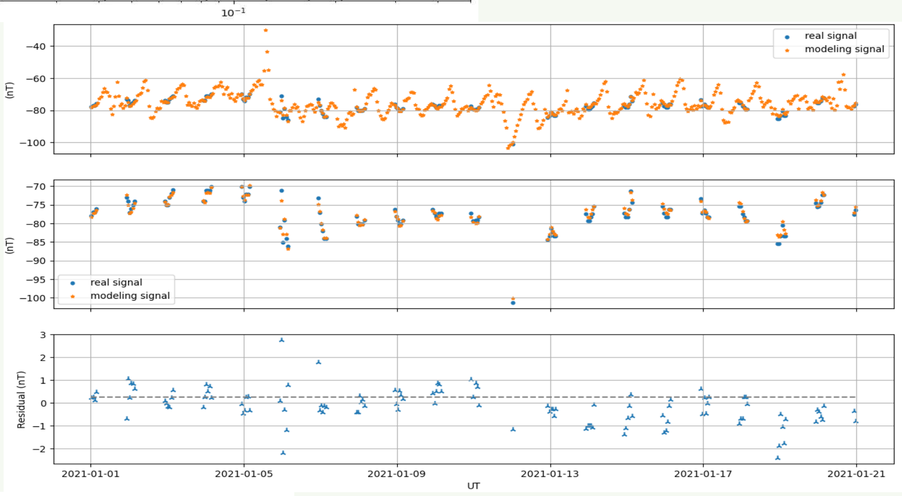

Figure 5: Example of the comparison between CLF (Chambon-la-foret) observatory data (in blue) and smoothed modeling signal (in orange) for x component over 20 days, the dotted grey line represent the annual average residue between observatory data and modeling signal

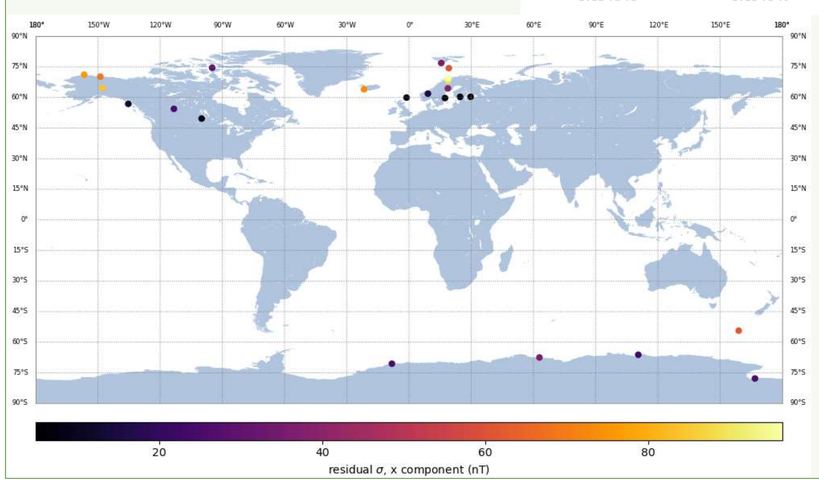

The distribution of residuals over year 2021 for each component at each observatory is calculated. Most of observatories have an annual average residual nearby 0 nT and an annual residual standard deviation smaller than 10 nT, except some observatories located at high latitudes shown in figure 6 where the residual standard deviation can reach 90 nT

Figure 6: Distribution of the 23 geomagnetic observatory positions with annual residual standard deviariations greater than 10 nT (σ>10nT) between observatory data and modeling signal